nature nanotechnology

SUPPLEMENTARY INFORMATION

DOI: 10.1038/NNANO.2014.32

Biogenic gas nanostructures as ultrasonic molecular reporters

Mikhail G. Shapiro*, Patrick W. Goodwill, Arkosnato Neogy, Melissa Yin, F. Stuart Foster, David V. Schaffer, Steven M. Conolly

CONTENTS

Supplementary Detailed Methods

Gas vesicle preparation. *Anabaena flos-aquae* (*Ana*, strain 1403/13F, CCAP, Argyll, Scotland) was cultured in sterile Gorham's media at room temperature under office fluorescent lighting with an approximately 75% circadian duty cycle. *Halobacteria NRC-1* (*Halo*, Carolina Biological Supply, Burlington, NC) was cultured at 37°C in high-salt medium (ATCC medium 2185), under ambient light, with rotation shaking at 225 rpm. GVs were isolated from *Ana* and *Halo* using hypertonic and hypotonic lysis, respectively (for 1 hour at room temperature), and purified by centrifugally-assisted flotation at 300 rcf (Supplementary Fig. S8) Hypertonicity was achieved by adding sucrose to a final concentration of 25%. Hypotonicity was implemented by diluting cells with a >8x volume of low-salt buffer (10mM Tris-HCl, 2.5mM MgCl2, 0.5mM CaCl2, pH7.6). To achieve purity (> 6,400X enrichment vs. non-buoyant cellular components), the harvested GVs were twice resuspended in > 80X volumes of phosphate-buffered saline (PBS) and re-centrifugated as above. This procedure is illustrated in Supplementary Fig. 5. GVs were diluted to experimental concentrations using PBS. To prepare pre-collapsed GVs, GV solutions were loaded into capped plastic syringes and the plunger depressed until the initially opaque solution (due to light scattering by intact GVs) became translucent (due to absence of light scattering by collapsed GVs).

The concentration of GVs was estimated based on their optical density (OD). Solutions of intact GVs appear milky white due to the scattering of light by their gas compartments[1]. GV collapse eliminates this light scattering, making it possible to subtract background contributions to the solution OD, yielding the "pressure-sensitive" OD at 500 nm ($OD_{500,PS}$). The relationship between $OD_{500,PS}$ and protein concentration (in mg/mL) was determined empirically using a total protein assay (micro-BCA kit, Pierce, Rockford, IL) performed on GVs purified as described above. Literature-based estimates of the molecular weight of the GVs (107 MDa for *Ana*, 686 MDa for *Halo*) [2-4] were used to calculate the molar concentration. We obtained a value of 564.2 ± 94.2 pM/ $OD_{500,PS}$ (N=5) and 16.1 ± 3.2 pM/ $OD_{500,PS}$ (N=3) for *Ana* GVs and *Halo* GVs, respectively, which we rounded up to 600 and 20 pM/ $OD_{500,PS}$, respectively. The value for *Ana* GVs is slightly higher than ~450 pM/ $OD_{500,PS}$ which can be calculated from literature, the discrepancy possibly arising from incomplete GV purity, the presence of popped GVs in the OD measurement and/or differences in the protein assays used. Gas volume fractions were estimated using approximate gas volumes of 8.4 µL per mg and 12.3 µL per mg for *Ana* and *Halo* GVs, respectively, derived from literature[3, 4].

For experiments comparing intact and lysed cells, concentrated *Ana* cultures (cell OD_{600nm} ~ 2) were mixed 50:50 with either water or 50% sucrose for 60 minutes, then loaded into ultrasound imaging gels as described above. To measure GV release upon lysis, $OD_{PS,500}$ was measured in solutions of lysed cells and compared to the dry pellet weight of paired cell samples (dry pellets were obtained by hydrostatically collapsing GVs inside the cells, pelleting the cells, washing with water, re-pelleting and drying overnight at 80ºC).

Bio-functionalization and aggregation. *Ana* GVs were biotinylated using EZ-Link Sulfo-NHS-LC-Biotin (Thermo Scientific, Rockford, IL) following supplier instructions, with a 10,000-fold molar excess of functionalizing reagent per GV, and purified by 3X repeated floatation (as in Supplementary Fig. S5c). For aggregation experiments, biotinylated GVs were mixed with streptavidin (G-Biosciences, St. Louis, MO) at indicated molar ratios and allowed to react for approximately 30 minutes before imaging.

In vitro ultrasound imaging. Imaging phantoms were prepared by casting 1% agarose gel (in water) around 96-well PCR reaction tubes, which were removed after solidification. 2X concentrated GV samples were mixed 1:1 with melted 1% agarose, and 100uL of the mixture was quickly loaded into phantom wells. The same procedure was used to load polystyrene microspheres (0.83% final w/v, 4.78 µm, Spherotech, Lake Forest, IL). After all samples have been loaded and solidified, additional 1% agarose was deposited to completely fill the wells and provide a uniform top surface. Imaging was performed using a home-built imaging setup. A 5 MHz, 10 MHz or 20 MHz single element transducer (6.3, 6.3 and 3.2 mm active areas, respectively; 25.4 mm focal distance; Olympus, Waltham, MA) was mounted on a computer-controlled 2D translating stage (VelMex, Bloomfield, NY). Transducer output was calibrated using a hydrophone (HGL-0200, Onda, Sunnyvale, CA). Phantoms were placed in a water container such that transducers could be immersed in the water at a distance of approximately 20 mm above the phantom. A programmable pulse generator (AFG3102, Tektronix, Beaverton, OR) and radio frequency amplifier (BT00500-AlphaS- CW, Tomco, Stepney, Australia) were used to drive transducers at specified frequencies with sinusoidal pulse trains of approximately 1 µs. The pre-amplifier function of a pulse-receiver (Pa-

nametrics/Olympus 5601A/TT) with high-pass and low-pass filtering at 5 MHz and 75 MHz, connected to an oscilloscope (Infiniivision DSOX2004A, Agilent Technologies, Santa Clara, CA; or LeCroy WaveJet 314, Chestnut Ridge, NY) was used to collect ultrasound signals and record them using MATLAB (Mathworks, Natick, MA). *In situ* GV collapse was obtained by repeated pulsing at indicated pressures with a 10 MHz transducer operating at 8 or 8.6MHz. Specific imaging parameters for each figure are listed in Supplementary Table S1.

Image analysis. Image analysis was performed in MATLAB. Raw time-domain signals acquired at each scan point were bandpass-filtered with symmetric Butterworth filters around the transmit or harmonic frequency, as indicated in Supplementary Table S1. After filtering, signals were brought back to baseband and time-gain compensation was applied using an empirically determined exponential coefficient. Line intensity profiles were obtained as the absolute value of a five point convolution of the in-phase and quadrature signal components. The resulting line intensity profiles were placed into arrays to generate two-dimensional B-mode images. The time axis was converted to space using the speed of sound in aqueous media (1540 m/s). If multiple neighboring lines perpendicular to the B-mode image were acquired, they were added together for averaging, as indicated in Supplementary Table S1. The resulting images were auto-scaled for presentation as indicated in Supplementary Table S1. Signals from regions of interest in each image were summated and used to generate quantitative plots. The regions of interest were defined manually in the axial dimension to include the contents of sample wells, and were defined automatically in the lateral dimension by detecting minima in axially integrated line intensity profiles and setting these minima as boundaries separating samples; the fidelity of automatically detected ROIs was always confirmed visually (and found not to require adjustment). Additional processing parameters are listed in Supplementary Table 1. Colour maps used in the images are shown in Supplementary Fig. S9. Power spectra represent squared absolute values of fast Fourier transforms of raw time-domain signals from regions of interest corresponding to wells containing GVs or polystyrene (Fig 2a. is the average of 48 such spectra).

In vivo imaging. All animal protocols were approved by the Animal Care and Use Committee of the University of California at Berkeley and the Animal Care Committee of Sunnybrook Research Institute, as appropriate. For imaging of subcutaneously injected GVs, female CD-1 mice, maintained under isoflurane anesthesia throughout the experiment, were depilated above the lower abdomen and injected subcutaneously with 150uL *Halo* GVs (OD 6) on one side and 150uL PBS on the other side of the abdomen. Placed on their backs, the mice were fitted with a homemade container allowing a ~3 cm column of ultrasound gel (Aquasonic, Parker Laboratories, Fairfield, NJ) to be placed above the injected region. An abdominal constriction was used to reduce breathing-related motion of the lower abdominal region. An ultrasonic transducer was coupled into the gel and scanned or used to apply destructive pulses as described above. To image animal anatomy (e.g., Fig. 4a), the pulse generation function of the pulse-receiver was used in place of the signal generator/amplifier. Additional scan parameters are listed in Supplementary Table S1.

Intravenously injected GVs were imaged in SCID nude mice using the VisualSonics Vevo 2100 high frequency ultrasound scanner operating in non-linear contrast mode, with the MS250 transducer set to 18 MHz and 2% power. The mice were maintained under isoflurane anesthesia and placed in supine position on a heated imaging platform. Breathing and heart rate were monitored by built-in sensors. The transducer was positioned above the abdomen such that the field of view would include the liver and the inferior vena cava. During infusion experiments, images were acquired continuously at a frame rate of 15frames/sec for approximately 100 seconds. 50 µL of *Halo* GVs in PBS at the indicated concentrations were infused approximately 10 seconds after the start of the experiment at a flow rate of 0.6 mL/min. After 65 seconds, a burst pulse (100% power) was applied for 1 second to collapse the GVs. To quantify contrast, ROIs encompassing the inferior vena cava and liver were drawn manually in the Vevo Lab software (for example, see Supplementary Fig. S10), and the averaged non-linear contrast signal within each ROI for each frame was exported into MATLAB for further analysis. Smoothed infusion time course curves were generated from the raw signal using a locally weighed scatterplot smoothing algorithm[5], which was further used to obtain pre-infusion, peak, steady state, and post-burst intensity values. To obtain AUC values, raw data was normalized to the average pre-infusion baseline, and positive signal values preceding the burst pulse were summated.

Halo GVs remaining in the liver following intravenous injection were imaged as described in the preceding paragraph, with the additional collection of images during 30-second windows at 15, 30, 45, 60

and optionally 75 minutes after injection. The liver signal in each image was quantified using ROI analysis as described above.

To image the persistence of *Halo* GV contrast after subcutaneous injection, 100 µL OD 6.0 *Halo* GVs were injected subcutaneously on the right side of the abdomen of a SCID nude mouse and 100 µL PBS was injected subcutaneously on the left side. The mouse was imaged using the Vevo 2100 system as described above. Images were collected immediately after injection and every 15 minutes thereafter for 120 minutes. A high-pressure burst pulse was applied to collapse any GVs still present after 120 minutes and imaged again.

Veterinary evaluation. The health of animals injected intravenously with OD 6.0 *Halo* GVs or PBS was evaluated by a veterinarian at Sunnybrook Research Institute on a 15-point scale comprising three points each for activity, weight, food intake, posture and hydration. The veterinarian was blinded to the injection group.

Transmission electron microscopy (TEM). TEM images were obtained on a Philips/FEI (Hillsboro, OR) Tecnai 12 microscope operating at 120kV. 10X diluted GV samples (from starting OD 1.0) were deposited on a carbon-coated formvar grid and negatively stained with 2% uranyl acetate in preparation for TEM imaging.

Supplementary Table S1 – Image Acquisition and Analysis Parameters

Figure	Transmit Frequency	Pulse Source	Peak Pressure	Pulse Train (us)	Averages / line	Perpendicular averages (distance)	Analysis Center Frequency	Analysis Bandwidth	Color map	Color map max	Color map min
1d – top	17Mhz	SG	175kPa	1µs	512	3 (1mm)	17MHz	4MHz	Hot	40X STD of PBS well	0
1d – middle	8.6Mhz	SG	189kPa	1µs	512	3 (1mm)	8.6MHz	4MHz	Hot	10X STD of PBS well	0
1d – bottom	4.8Mhz	SG	148kPa	1µs	512	3 (1mm)	4.8MHz	4MHz	Hot	10X STD of PBS well	0
1e - top	17Mhz	SG	175kPa	1µs	512	3 (1mm)	17MHz	4MHz	Hot	40X STD of PBS well	0
1e-middle	8.6Mhz	SG	189kPa	1µs	512	3 (1mm)	8.6MHz	4MHz	Hot	10X STD of PBS well	0
1e - bottom	4.8Mhz	SG	148kPa	1µs	512	3 (1mm)	4.8MHz	4MHz	Hot	10X STD of PBS well	0
2b - top	6MHz	SG	98kPa	1µs	512	3 (1mm)	6MHz	4MHz	Hot	0.7X MI	0
2b - middle	6MHz	SG	98kPa	1µs	512	3 (1mm)	12MHz	4MHz	Hot	MI	0
2b - bottom	6MHz	SG	98kPa	1µs	512	3 (1mm)	18MHz	4MHz	Hot	MI	0
2d - top	8.6MHz	SG	166kPa	1µs	512	3 (1mm)	8.6MHz	4MHz	Hot	0.7X MI	0
2d - middle	8.6MHz	SG	166kPa	1µs	512	3 (1mm)	8.6MHz	4MHz	Hot	0.7X MI of 2d top	0
2d - bottom	Calculated								Hot	0.7X MI of 2d top	0
2f	8.6MHz	SG	166kPa	1µs	512	3 (1mm)	8.6MHz	4MHz	Hot	0.5 MI	0
2g,h-magenta	Calculated from data shown in Fig. 2f.								Magenta	0.8X MI	0
2g,h - green	Calculated from data shown in Fig. 2f.								Green	0.4X MI	0
3b	17MHz	SG	77kPa	1µs	64	1	17MHz	4MHz	Hot	MI	0
3f	17MHz	SG	77kPa	1µs	64	1	17MHz	4MHz	Hot	MI	0
4a - gray	10MHz transducer	PR	Power setting 4	n/a	512	3 (0.1mm)	10MHz	10MHz	Gray	0.2X MI	0
4a - green	6MHz	SG	85kPa	1µs	512	3 (0.1mm)	12MHz	4MHz	Black to green	0.35X MI	0.14X MI
4b, c	6MHz	SG	85kPa	1µs	512	3 (0.1mm)	12MHz	4MHz	Hot	0.7X MI	0.035 X MI
4e-i	18MHz	Vevo	2% power	n/a	n/a	n/a	Contrast mode	n/a	Vevo std.	Vevo std.	Vevo std.
Sup. S1	17Mhz	SG	175kPa	1µs	512	3 (1mm)	17MHz	4MHz	Hot	100X avg. intensity of PBS	0
Sup. S2	17MHz	SG	175kPa	1µs	512	3 (1mm)	17MHz	4MHz	Hot	Scaled to show shadowing	0
Sup. S4 a, d, g, j, m	10MHz transducer	PR	Power setting 4	n/a	512	3 (0.1mm)	10MHz	10MHz	Gray	0.2X MI	0
Sup. S4 b,c,e,f, k, l, n, o	6MHz	SG	85kPa	1µs	512	3 (0.1mm)	12MHz	4MHz	Hot	0.7X MI	0.035 X MI
Sup. S4 h, i	6MHz	SG	85kPa	1µs	512	3 (0.1mm)	12MHz	4MHz	Hot	0.5X MI	0.025 X MI

Abbreviations: SG – Signal generator, PR – Pulse receiver, Vevo – Vevo 2100 ultrasound scanner; STD – Standard deviation, MI – Maximum intensity

Supplementary Table S2 – Gas Vesicle Toxicity Assessment

	GVs	Saline
Pre	15	15
Post	15	15
24h	14.7±0.3	15
48h	15	15

Supplementary Table S2 - Gas vesicle toxicity assessment. Mean health grades of mice injected intravenously with 50µL OD 6.0 *Halo* GVs or PBS. Mice were scored on a 15-point scale comprising 3 points each for activity, weight, food intake, posture and hydration by a veterinarian blinded to injection group. Evaluations were performed before, immediately after and 24 and 48 hours after injection. (N=3, ±SEM). Only one mouse (at 24h) scored less than 15 points due to a minor drop in weight (resulting in a 14/15 score), and recovered by 48h.

Supplementary Figure S1

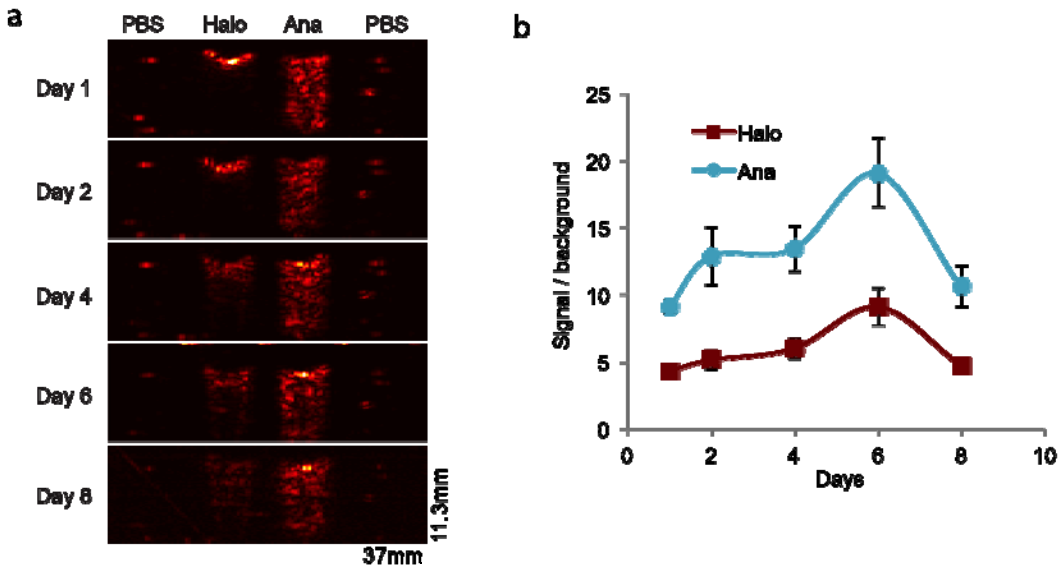

Supplementary Figure S1. Gas vesicle longevity. a, Ultrasound image (17 MHz pulses) of a phantom containing PBS buffer, OD 2.0 *Halo* GVs, OD 2.0 *Ana* GVs or another well of PBS buffer, acquired repeatedly over several days, as indicated. Note that the intensity profile of *Ana* GVs shows minimal change. *Halo* GV signal appears to show less of a shadowing effect, potentially indicative of a decrease in *Halo* GV concentration. **b**, Total backscattered signal from *Halo* and *Ana* GVs on each day of sampling, relative to PBS controls (N=4/sample). Detailed image acquisition and analysis parameters are provided in Supplementary Table S1; colour map in Supplementary Fig. S6. Error bars represent ± SEM. The size of the field of view is indicated in the lower right corner of the bottom image.

Supplementary Figure S2

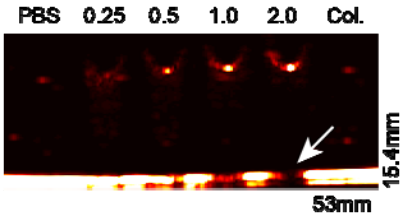

Supplementary Figure S2. Attenuation effect from *Halo* gas vesicles. Ultrasound image (17MHz) of phantom containing PBS buffer, *Halo* GVs at indicated optical densities or collapsed OD 2.0 *Halo* GVs. The intense signal at the bottom of the image corresponds to the solid bottom of the imaging phantom. The arrow points to a location underneath *Halo* GVs where the signal from the solid bottom is attenuated. Smaller attenuation can be observed at lower concentrations of GVs. Detailed image acquisition and analysis parameters are provided in Supplementary Table S1; colour map in Supplementary Fig. S6. The size of the field of view is indicated in the lower right corner of the bottom image.

Supplementary Figure S3

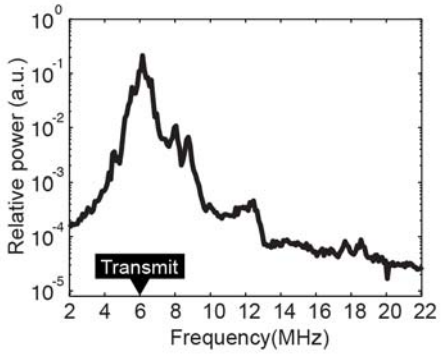

Supplementary Figure S3. Harmonic ultrasound response of *Ana* GVs. Power spectrum of signal backscattered from OD 2.0 *Ana* GVs in response to 6 MHz ultrasound pulses (peak amplitude 98 kPa). Each point represents an average of 16 measurements.

Supplementary Figure S4

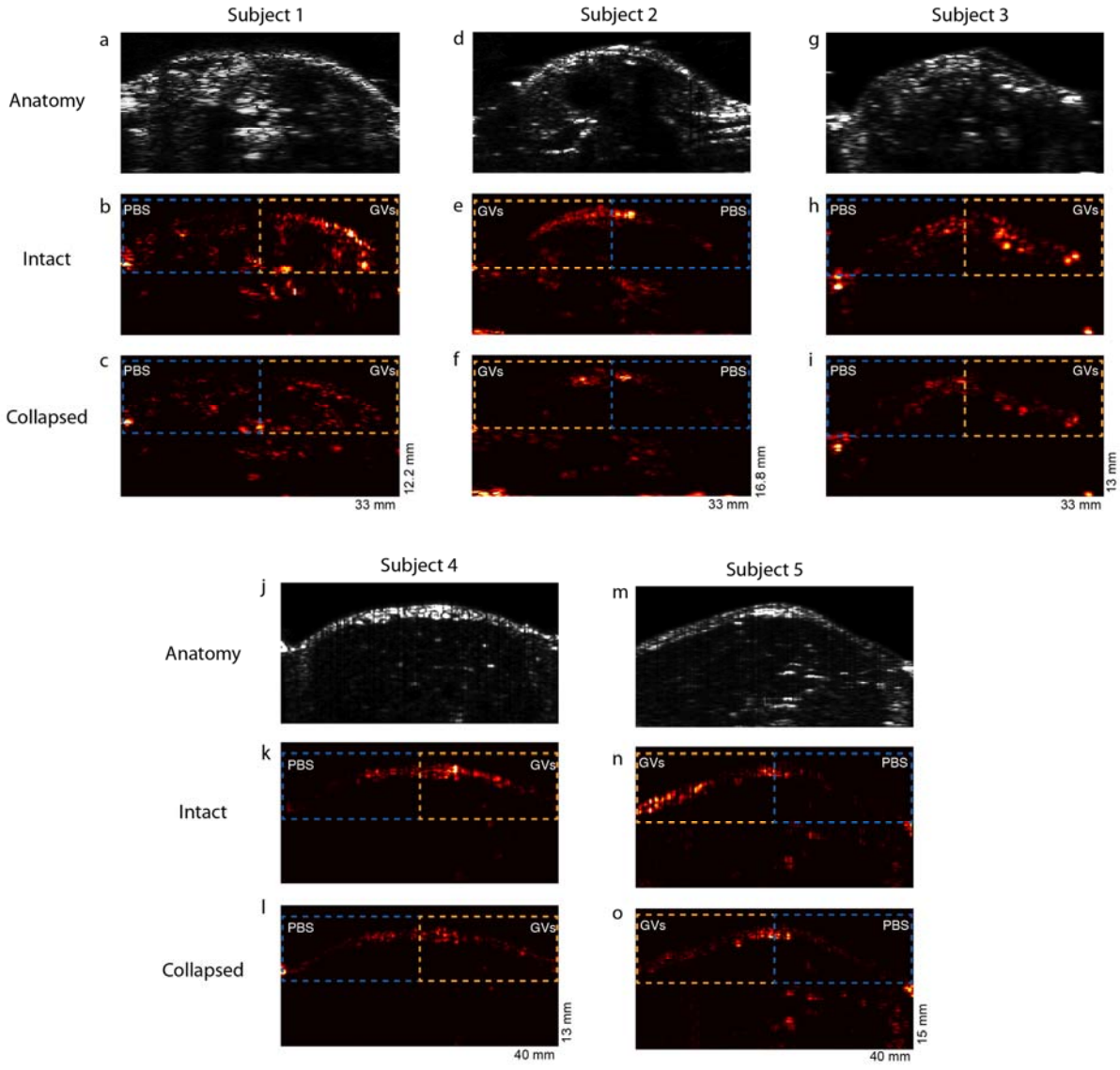

Supplementary Figure S4. Gas vesicle imaging *in vivo*. a, Three mice were depilated and injected subcutaneously with 150uL OD 6.0 *Halo* GVs or 150uL PBS on opposite sides of the abdomen, as indicated. **a, d, g, j m.** Anatomical ultrasound images acquired with 10MHz transducer. **b, e, h, k, n.** 12MHz harmonic ultrasound images (6MHz pulsing) **c, f, i, l, o.** 12MHz harmonic ultrasound images after GV collapse with destructive insonation. Dashed ovals indicate approximate location of injected material. Subject 1 is also shown in Figure 4. Detailed image acquisition and analysis parameters are provided in Supplementary Table S1; colour maps in Supplementary Fig. S6. The size of the field of view is indicated in the lower right corner of the bottom image.

Supplementary Figure S5

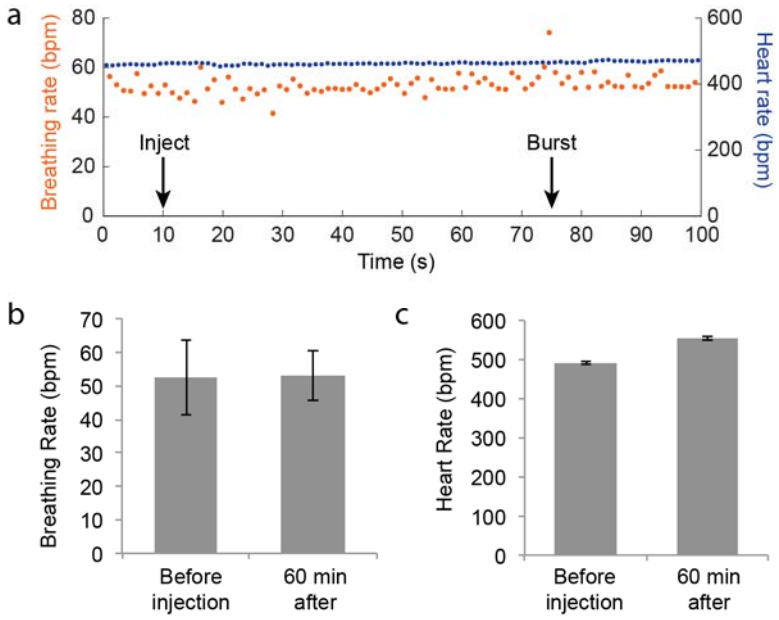

Supplementary Figure S5. Effect of gas vesicle injection on heart rate and breathing. a. Heart rate and breathing rate recorded during a *Halo* GV injection such as the one shown in Fig. 4, h. Arrows indicate the approximate timing of GV injection and the burst pulse. **b-c.** Mean heart rate (b) and breathing rate (c) measured immediately before and 60 min after intravenous injection of 50µL OD 6.0 *Halo* GVs. N=4. Error bars ± SEM.

Supplementary Figure S6

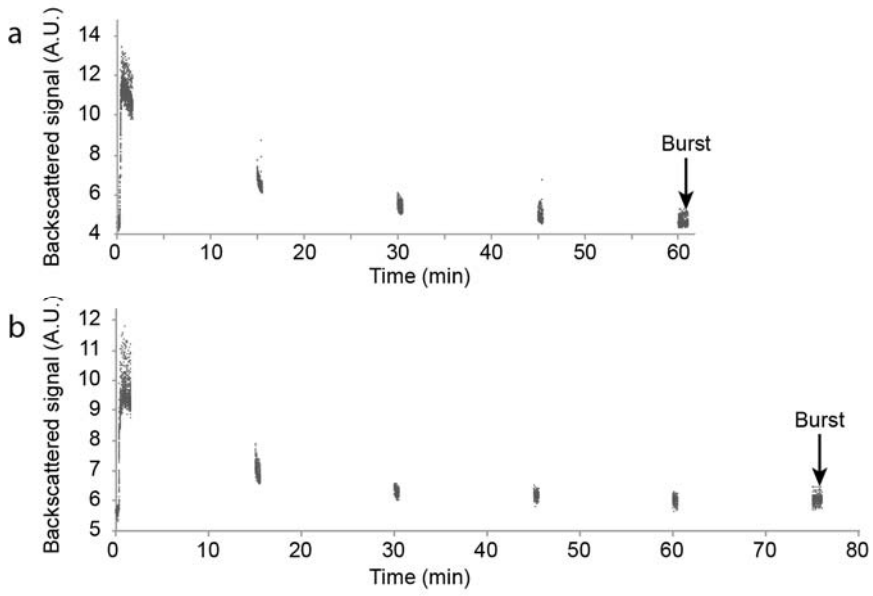

Supplementary Figure S6. Gas vesicle clearance in the liver. Backscattered non-linear signal in the livers of two mice (shown in **a** and **b**) injected intravenously with OD 6.0 *Halo* GVs. Injection, imaging parameters and ROI analysis were the same as for Fig 4, e-h, except that mice were kept anesthetized for 60-80 minutes after injection with imaging repeated every 15 minutes, as shown. At either 60 (a) or 75 (b) minutes after injection, a high-pressure burst pulse was applied to collapse any remaining GVs (as indicated by arrows).

Supplementary Figure S7

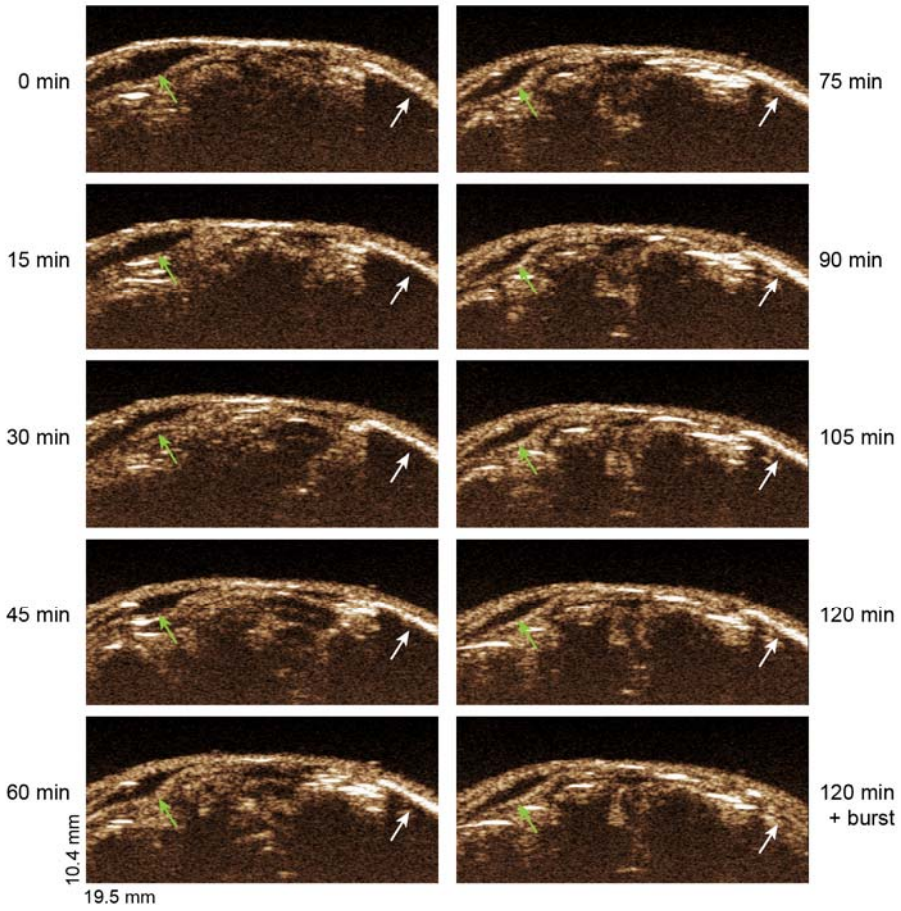

Supplementary Figure S7. Persistent gas vesicle signal after subcutaneous injection. Non-linear contrast images of SCID nude mice injected subcutaneously with 100 µL OD 6.0 *Halo* GVs (right side) or 100 µL PBS buffer (left side), acquired using a high-frequency ultrasound scanner system operating at 18 MHz and 2% power. The images were taken immediately after injection and every 15 minutes thereafter as indicated next to each image. A high-pressure burst pulse was applied to collapse the GVs still present after 120 minutes, resulting in the bottom right image. The white arrow denotes contrast attributed to GVs (and its absence after the burst pulse). Note that the GVs show up as a bright anterior line of robust echogenicity with strong shadowing of the distal tissue below it due to attenuation (consistent with Supplementary Fig. S2). Brightening of the GV signal during the first hour of imaging is attributed to absorption of the PBS fluid in which the GVs are injected, increasing their local concentration; absorption of the fluid pocket is also observed on the control side. Both the highly echogenic signal and the shadowing are eliminated by the burst after 120 min. The green arrow indicates the expected location of the injected PBS.

Supplementary Figure S8

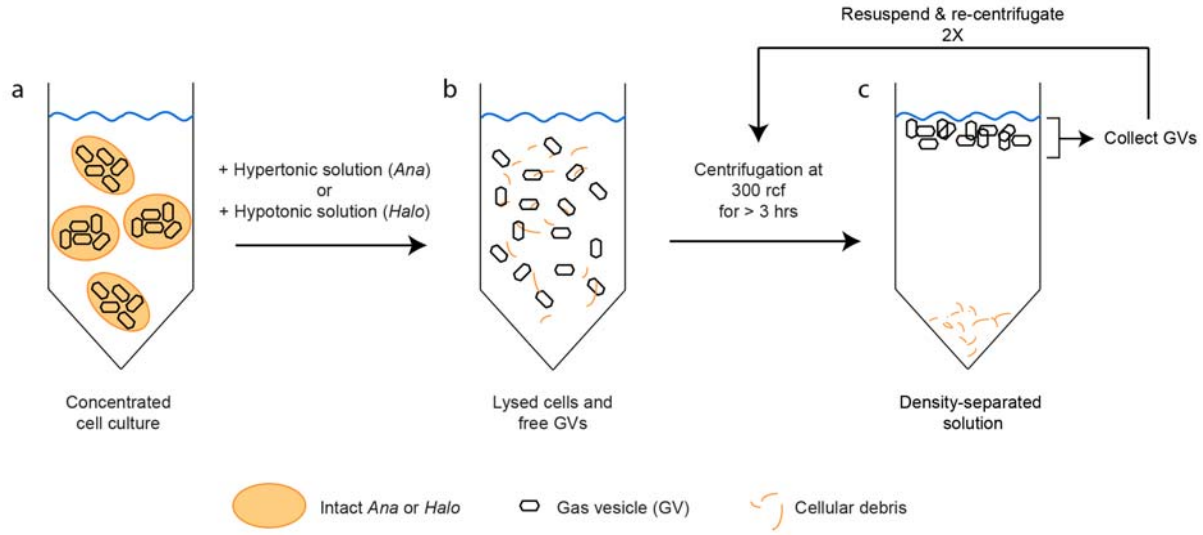

Supplementary Figure S8. Gas vesicle purification from *Ana* and *Halo* cells. GVs are purified through tonic lysis of cells followed by centrifugally-assisted floatation. **a.** Concentrated suspensions of *Ana* or *Halo* cells are disrupted through hypertonic lysis (addition of 25% sucrose) or hypotonic lysis (8-fold dilution in low-osmolarity buffer), respectively, for 1 hour. **b.** The resulting suspension is centrifugated for 3 hours or longer at 300 rcf (this low speed is chosen to prevent GV disruption by pressure). **c.** GVs are collected from the surface of the centrifugated solution, re-suspended in > 80X PBS and re-centrifugated. This step is repeated twice.

Supplementary Figure S9

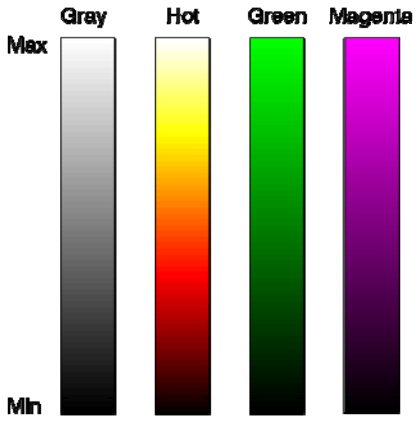

Supplementary Figure S9. Colour maps used in ultrasound images. Gray, Hot, Green and Magenta colour maps as used in Figs. 1-4 in the main text and Supplementary Figs. S1, S2 and S4. The scales are linear between Min and Max. The colour map used and the values of Min and Max are defined for each image in Supplementary Table S1. The colour maps Gray and Hot are standard in MATLAB. Green and Magenta were prepared by replacing the color white with either green or magenta in the Gray color map.

Supplementary Figure S10

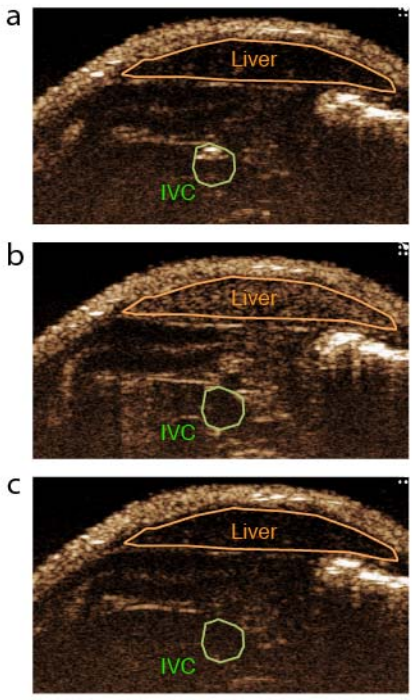

Supplementary Figure S10. Representative regions of interest used to generate Fig. 4, h-l. Non-linear contrast images showing representative regions of interest (ROIs) for the liver and inferior vena cava (IVC), which were used to generate the data shown in Fig. 4, h-l.

Supplementary References

1. Walsby, A.E. Gas vesicles. *Microbiol. Rev.* **58**, 94-144 (1994).
2. Jost, M., Jones, D.D. & Weathers, P.J. Counting of gas vacuoles by electron microscopy in lysates and purified fractions of microcystis aeruginosa. *Protoplasma*, 329-335 (1971).
3. Walsby, A.E. & Armstrong, R.E. Average thickness of the gas vesicle wall in Anabaena flos-aquae. *J. Mol. Biol.* **129**, 279-285 (1979).
4. Yao, A.I. & Facciotti, M.T. Regulatory multidimensionality of gas vesicle biogenesis in Halobacterium salinarum NRC-1. *Archaea* **2011**, 716456 (2011).
5. Cleveland, W.S. Robust locally weighted regression and smoothing scatterplots. *J. Am. Stat. Assoc.* **74**, 829-836 (1979).